Incipient Fault Diagnosis of Roller Bearing using Optimized Wavelet Transform based Multi-speed Vibration Signatures

Zhiqiang Huo[1,2], Yu Zhang[1], Pierre Francq[3], Lei Shu[1,2*], Jianfeng Huang[2]
[1]School of Engineering, University of Lincoln, Lincoln, UK
[2]Guangdong Provincial Key Laboratory on Petrochemical Equipment Fault Diagnosis,
Guangdong University of Petrochemical Technology, Maoming, China
[3]Mines Albi, University of Toulouse, Toulouse, France
Email: {zhuo, yzhang, lshu}@lincoln.ac.uk, pierre.francq@mines-albi.fr, jianfeng.huang@outlook.com

***Abstract*—Condition monitoring and incipient fault diagnosis of roller bearing is of great importance to detect failures and ensure reliable operations in rotating machinery. In this paper, a new multi-speed fault diagnosis approach is presented by using self-adaptive wavelet transform components, generated from bearing vibration signals. The proposed approach is capable of discriminating signatures from four conditions of roller bearing, i.e. normal bearing and three different types of defective bearings on outer race, inner race and roller separately. Particle Swarm Optimization (PSO) and Broyden-Fletcher-Goldfarb-Shanno (BFGS)-based quasi-Newton minimization algorithms are applied to seek for optimal parameters of the Impulse Modelling based Continuous Wavelet Transform (IMCWT) model. Consequently, a three-dimensional feature space composed of statistical parameters and a Nearest Neighbor (NN) classifier are respectively applied for fault signature extraction and fault classification. Effectiveness of this approach is then evaluated, and the results have achieved an overall accuracy of 100%. Finally, the experimental outcomes have proven that the generated discriminatory fault signatures are suitable for representing multi-speed fault data sets. This technique will be further implemented and tested in a real industrial environment.**

***Index Terms*—Fault diagnosis, Vibration measurement, Continuous wavelet transforms, Roller bearing, Particle swarm optimization, Quasi-Newton minimization, Fault signatures**

I. Introduction

Roller bearings have been used extensively in industrial environments, where they play a vital role designed for supporting constrained relative rotation and reducing friction between two parts used for transformation of energy. The service life of a roller bearing is normally determined by material fatigue, corrosion, and wear at the running surface. Insights into incipient Fault Detection and Diagnosis (FDD) and predictive maintenance are conducive to alleviate the negative impacts of latent performance degradation and proactively provide administrators with the real-time machines' operating conditions. In the last decades, incipient FDD of roller bearing has attracted a great deal of attention attempting to effectively monitor, diagnose, and isolate bearing faults with the purpose of reducing less down-time and financial losses in industrial factories [1].

Corresponding author: Lei Shu (email: lshu@lincoln.ac.uk)

In recent decades, great efforts have been devoted to the field of fault diagnosis of roller bearing with a variety of condition monitoring methods, such as acoustic emission, vibration, temperature, and electronic current monitoring methods [2], [3]. Among those approaches, the vibration signals, depicted as machine's signature, particularly enjoy the inherent capability of characterizing typical vibration levels and specific frequency spectrums generated from rotating components. In practice, vibrations are caused by the transmission of cyclic forces which in fact are behaviors of energy loss. Defective roller bearings therefore gradually generate various forces causing high amplitude of vibration leading to aggravating energy consumption. For instance, in a specific case of a water pumping station bearing faults would increase vibration level up to 85%, where power consumption increases 14% and pump efficiency decreases 18% [4]. Most importantly, with the advent of accelerometer sensor, collecting data has currently become a simple exercise that helps to provide a wide dynamic range and frequency range for vibration measurement, which has been found to be highly reliable, versatile, and accurate.

During the last decades plenty of techniques for FDD of roller bearing have been further studied to establish a firm position based on vibration signal processing. In general, steps of FDD can be mapped into three phrases: data acquisition, feature extraction, and fault classification, and the later two are the priority. The vibration data as initial input is supposed to be correctly operated and measured to reflect equipment's intrinsic behaviors. Feature extraction [5] is regarded as the key step that transforms input data into a reduced set of features which contain critical, compressed, and characteristic information. Afterwards artificial intelligence-based classification techniques can be used to distinguish different conditions of bearing, before which signal processing techniques are needed to be applied to reduce the magnitude and the redundant information in original vibration signals. Fast Fourier Transform (FFT) and Short Time Fourier Transform (STFT)

are two approaches for signal decomposition by converting the time-domain contents into frequency spectrum [6]; however, it has been emphasized that it may probably lower down the decomposing performance based on FFT and STFT since inappropriate time windows adopted in these methods [7] that may be not efficient enough for analyzing non-linear and non-stationary signals.

In supplement, a great deal of data-driven models have been further studied to establish a firm position in signal processing. Among those, wavelet analysis is one of the most powerful signal processing techniques which enjoys high resolution in both time and frequency domain [8], [9]. To be more specific, the wavelet analysis has good time and poor frequency resolutions at high frequencies, and good frequency and poor time resolutions at low frequencies. Verifying window size allows the possibility to extract valuable information from vibration signals. Continuous Wavelet Transform (CWT), one efficient wavelet method, uses groups of non-orthogonal wavelet frames to generate general symptoms, which enjoys the ease of interpretation at the cost of saving space. In addition, with the advent of artificial intelligent methods, plenty of techniques have been successfully employed in the field of FDD based on CWT analysis (e.g., Artificial Neural Networks (ANNs), and Support Vector Machine (SVM)). Various artificial intelligence techniques are used along with wavelet transform for fault diagnosis in rotating machinery [10]–[12]. As an example, Jafar et al. [13] proposed a method for diagnosis of roller bearings based on ANNs. In this method, vibration signals firstly passed through Removing Non-bearing Fault Component (RNFC) filter, and then were fed into another neural networks for fault classification. Similarly, Kankar et al. [14] presented an approach for FDD of roller bearings by using three machine learning methods, namely SVM, ANN, and Self-Organizing Maps (SOM). The results showed that SVM and ANN outperformed better than SOM in classification success rate. Apart from that, Lou et al. [15] introduced a new scheme for the diagnosis of localized bearing defects based on wavelet transform and neuro-fuzzy classification. In [16] a hybrid method based on CWT and SVM was proposed for detecting defects in motor ball bearings.

It is needed to notice that although there are a number of diagnosis approaches for bearings based on wavelet analysis have been proposed, whilst it cannot be neglected that for achieving optimistic accuracy it usually involves a large number of parameters and aggravating computation burden. Apart from that, taking into account that non-stationary and non-linear features commonly exist in vibration signals, the predefined kernels may not completely guarantee the convergence to the characteristics of signals. There is still a need to design a new technique that utilizes optimized wavelet transform directly generated from original signals for multi-speed fault diagnosis of roller bearing in rotating machinery.

In this paper, the Impulse Modelling-based CWT (IMCWT) model is introduced for decomposing vibration signals obtained from roller bearings with wavelet transformation. To obtain optimal IMCWT model, PSO and Broyden-Fletcher-Goldfarb-Shanno (BFGS)-based quasi-Newton optimization algorithms are respectively used to optimize IMCWT model for global and local optimization purposes. After that, three-dimensional statistical parameters are applied to extract fault characteristics. Nearest Neighbor (NN) classifier using Mahalanobis distance is adopted to map samples into corresponding fault categories. Consequently, a novel intelligent fault diagnosis approach for roller bearings is presented with experimental validation by means of combining IMCWT decomposition, PSO and BFGS-based quasi-Newton optimization algorithms, three-dimensional feature extraction, and NN-based classifier using Mahalanobis distance evaluation.

The main contributions in this paper are concluded as follows:

- An optimized impulse modelling-based approach was proposed for wavelet analysis to characterize fault symptoms hidden in vibration signals measured from different conditions of roller bearing.
- In this paper, a hybrid approach for multi-speed fault diagnosis of roller bearing was proposed based on the optimized IMCWT model and statistical analysis with NN-based classifier using Mahalanobis distance.
- Statistical parameters were evaluated and compared by investigating their performances of speed sensitivity and discriminatory potentials to generate fault signatures under different rotating speeds.
- 2D and 3D fault signatures were generated in dimensional feature space. Meanwhile, the experimental outcomes showed that the proposed approach can be effectively used for generating both single and multi speed fault signatures based on vibration monitoring.

The rest of this paper is organized as follows: Section II introduces IMCWT model and describes parameter optimization method of IMCWT model using PSO and BFGS-based quasi-Newton minimization techniques. Section III presents the proposed fault diagnosis methodology for generating multi-speed fault signatures. Experimental validation, results and multi-speed fault signatures are given in Section IV. Finally, the conclusion of this paper is presented in Section V.

II. Proposed IMCWT Model

In this section, CWT is first briefly introduced. Afterwards, IMCWT is presented for decomposing the redundant original vibration signals of roller bearing. After that, the process of parameter selection and optimization of IMCWT model based on PSO and BFGS-based quasi-Newton optimization techniques are separately introduced.

A. Review of Wavelet Analysis

Problems of the time and frequency resolution commonly exist regardless of any transform applied in the process of decomposition. CWT was developed as an alternative approach to FFT and STFT so as to overcome the resolution problem, which decomposes different segments of a time-domain signal with adjustable window function. The CWT wavelet transform

is defined as follows:

$$CWT_x^{\psi}(\gamma, s) = \Psi_x^{\psi}(\gamma, s) = \frac{1}{\sqrt{s}} \int x(t)\Psi\left(\frac{t-\gamma}{s}\right) dt. \quad (1)$$

where $x(t)$ is the signal, s is the scale factor, γ is the translation parameter, $\Psi(t)$ is the wavelet transforming function, and it is also called the mother wavelet. The term wavelet represents the window function which has finite length. The term mother wavelet means that time functions transformed to map different segments of the signal are deserved from one major function. Similar to the frequency used in STFT, the parameters s and $\Psi(t)$ in the wavelet analysis are respectively used in the transforming operation of dilating and translating time function. To be more specific, large s value corresponds to non-detailed global view, and low s value corresponds to a detailed view of the segment of a signal. Particularly, the factor $\frac{1}{\sqrt{s}}$ is used to ensure energy preservation.

In general, wavelet analysis is one of the most powerful technique used for signal processing. Having been enjoyed the advantages of reliable and flexible abilities of generating general and fine-grained information extraction, CWT has been extensively proved that can be employed in the field of FDD for the analysis of non-stationary and non-linear signals.

B. Impulse Modelling based Continuous Wavelet Transform (IMCWT)

In practice, the response of the system to the instant δ-impulse in vibrodiagnostics can be represented using a pattern depicted as a response of the single-degree-of-freedom-system, which can be formulated as follows [17]:

$$f(x) = \alpha e^{-\beta x} cos(wx + \varphi) \quad (2)$$

where $f(x)$ is the displacement, α is the premier amplitude, and w is the resonance frequency, which is the frequency of the system fluctuation without resistance. Taking assumption that at the impulsive start the system was at rest into consideration, Eqs. (2) can be applied as a mother wavelet in CWT, which can be expressed as follows:

$$\Psi(t) = sin(\alpha t + \beta) e^{-\gamma|t|} \quad (3)$$

For keeping minimum parameters in the mother wavelet, this IMCWT model has three parameters that have the ability of representing a system's working state, which therefore can be employed into FDD of roller bearing. To optimize IMCWT model, global and local optimization techniques are used for parameter selection, which are presented in the following.

C. Parameter selection with global and local optimization

1) Glocal optimization: PSO: The selection of optimum parameters, in practical, has a great influence on predicting effectiveness of wavelet analysis. PSO, proposed by Kennedy and Eberhart [18], is a population-based global search algorithm, which was developed to optimize a problem by iteratively improve a candidate solution with regard to a given measure of quality. PSO, different from genetic algorithms, has no crossover and variation instead of using the optimal particle search in the solution space. To be more specific, PSO performs by iteratively using a population (called a swarm) of candidate solutions (called particles) in the search-space. The swarm consists of m numbers of particles, each of which has own velocity $v_{i,j}(t)$, current position $x_{i,j}(t)$, and local best known position $pbest_j(t)$ $(i = 1, 2, \cdots, m; j = 1, 2, \cdots, n)$. Each particle moves towards own best previous position and the best known positions found by other particles $gbest_j(t)$ in the search-space, which is expected to move the swarm towards the best solutions. The standard PSO can be performed according to the following equations:

$$\begin{aligned} v_{i,j}(t+1) =& w \times v_{i,j}(t) + c_1 \times r1() \times (pbest_j(t) - x_{i,j}(t)) \\ &+ c_2 \times r2() \times (gbest_j(t) - x_{i,j}(t)) \end{aligned} \quad (4)$$

$$x_{i,j}(t+1) = x_{i,j}(t) + v_{i,j}(t+1) \quad (5)$$

where j is the nth dimension of a particle $(1 \leq j \leq n)$, the velocity is restricted to the [-v_{max}, v_{max}] range, $r1()$ and $r2()$ are random numbers in the range of [0,1], $c1$ and $c2$ are positive constants corresponding to personal and social learning factors, and w is the inertia weight. In this paper, the initialized parameters with respect to the size of swarm, inertia weight, maximum number of iterations are selected as follows: swarm size $p = 20$, $c1 = 1.3$, $c2 = 1.75$, max stall iterations $t_{max} = 6$. The search range of α, β, γ is from [0, 0, 0] to [200, 200, 200].

2) Local optimization: BFGS-based quasi-Newton minimization: After generally searching optimized parameters by using global optimization, the BFGS-based quasi-Newton unconstrained minimization method is used to accurately locate minimum solutions for IMCWT model [19]. In local unconstrained minimization, the quasi-Newton method is one of the most favored optimization methods that uses curvature information at each iteration to formulate a quadratic model problem, which has the following form:

$$\min_{x \in R^n} f(x) = \frac{1}{2} x^T H x + b^T x + c \quad (6)$$

where H, the Hessian matrix, is a positive definite symmetric matrix, b is a constant vector, and c is a constant. This method has optimal solution when the partial derivatives of x approach to zero shown as below:

$$\bigtriangledown f(x^*) = Hx^* + c = 0 \quad (7)$$

The optimal solution, x^*, can be formulated as

$$x^* = -H^{-1}c \quad (8)$$

Different from Newton-type methods that directly calculate H, quasi-Newton method uses the observed behavior of $f(x)$ and its gradient to build up curvature information to properly update an approximation to H, which avoids a large amount of calculation. For Hessian updating, the BFGS

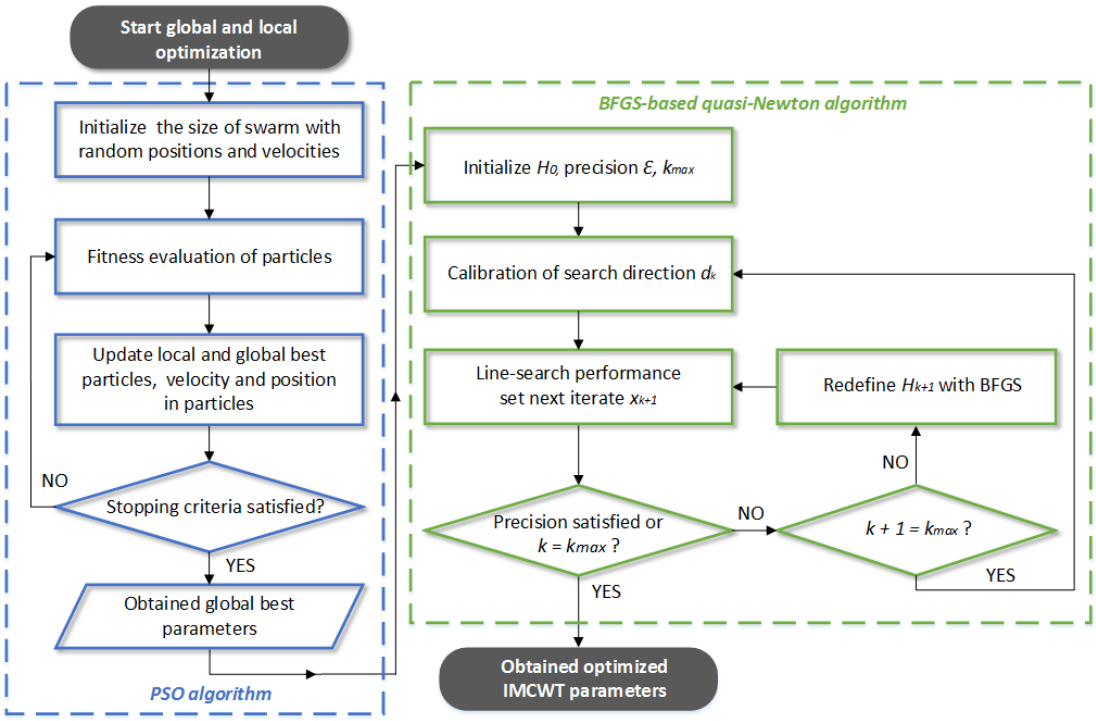

Fig. 1: The process of parameter selection for IMCWT model using PSO and BFGS-based quasi-Newton optimization.

is generally thought to be an effective method that can be used for iteratively optimizing the search direction. It's needed to notice that, in BFGS method, H is a positive definite matrix that generates a direction of descent, as a result of which for any steps with small value of the objective function decreases all the time. In BFGS, the formula for generating an approximation to H is described below:

$$H_{k+1} = H_k + \frac{q_k q_k^T}{q_k^T s_k} - \frac{H_k s_k s_k^T H_k^T}{s_k^T H_k s_k} \tag{9}$$

where s_k and q_k are formulated as following:

$$s_k = x_{k+1} - x_k \tag{10}$$

$$q_k = \bigtriangledown f(k_{x+1}) - \bigtriangledown f(x_k) \tag{11}$$

At the beginning of iterations, H_0 can be set to identify matrix I_0. This formula therefore can be used to make an approximation of the H^{-1} at each update to avoid a great deal of calculation. After that, line-search method is applied to locate the best solution, x_k, along the search direction by repeatedly minimizing polynomial interpolation models of the objective function. That it, the next iterate x_{k+1} has the following form:

$$x_{k+1} = x_k + \alpha^* d_k \tag{12}$$

where x_k is the current iterate, d_k is the search direction, and α^* is a scalar step length parameter. At each iteration, a line search is performed to locate the best solution in the given direction:

$$d_k = -H_k^{-1} \cdot \bigtriangledown f(x_k) \tag{13}$$

In this paper, BFGS-based quasi-Newton unconstrained minimization serves to locate optimized parameters after global optimization. The max number of iterations, t_{max}, is set to 80, and maximum number of function evaluations is 300.

3) The process of parameter selection using global and local optimization: In this study, for obtaining optimized IMCWT model, there are in total three parameters, namely α, β, γ needed to be evaluated. The process of parameter selection and evaluation with PSO and BFGS-based quasi-Newton algorithms is presented in Fig. 1, which is described below:

Step 1: initialization of global optimization. Randomly generate the initial position (corresponding to α, β, and γ) and velocity of each particle. Set the size of swarm, iteration variable $t = 0$, maximum iteration number t_{max}, and inertia weight $c1$, $c2$. Afterwards, start global training process from step 2 to 4.

Step 2: fitness evaluation. The fitness function is designed for evaluating current particles' performance, which is needed to be given before the start of optimization. In this paper trust rate is adopted to evaluate statistical similarity between the new sample and given classes, which is

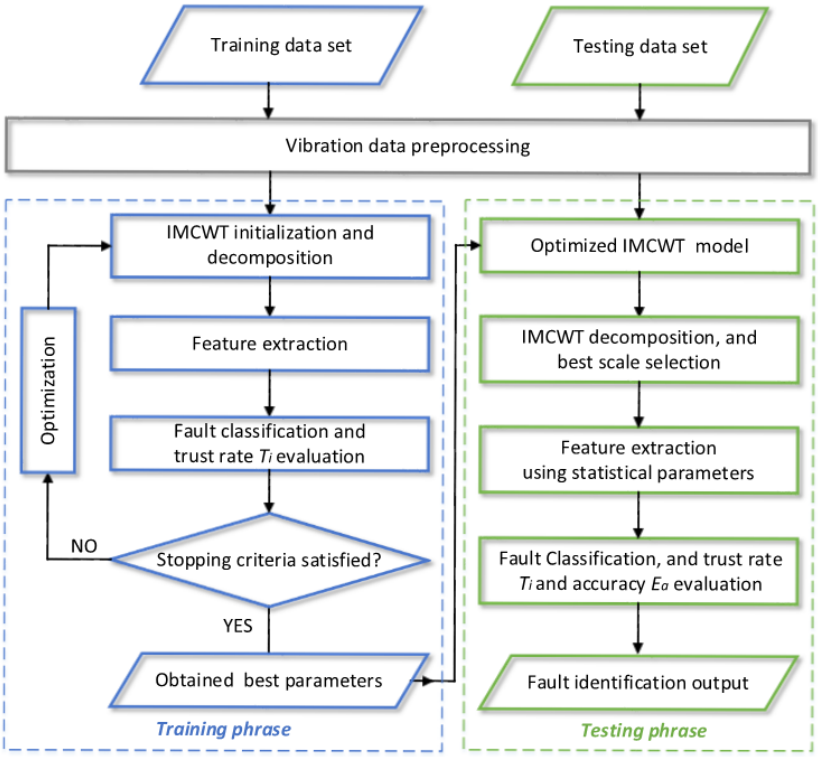

Fig. 2: Training and testing process of fault diagnosis for roller bearing using the proposed methodology.

defined as follows:

$$T^i_{trust} = \left(1 - \frac{d_i}{d_{min} + d_i}\right) \times 100\% \quad (i \in c) \qquad (14)$$

where i is the ith number of classes, d_i is the distance between ith class and the new sample. Particularly, since there are only four given fault types studied in this paper, the trust rate of the class with minimum distance can be achieved by using $100 - max(T^i_{trust})$. Afterwards, on the basis of trust rate evaluation, fitness function is formulated as below:

$$F_{fit} = -\bar{T}_{trust} = -\frac{\sum_{i=1}^{c} T^i_{trust}}{c} \qquad (15)$$

where c is the total number of classes, $\bar{T}_{trust}$ is the mean trust rate of c kinds of classes. From the above definition, it can be easily seen that the fitness decreases when trust rate increases. It is needed to notice that both PSO and quasi-Newton optimization techniques are minimization methods, the fitness value is supposed to decrease with higher classification accuracy. That is, the value of fitness tends to approach to a desired solution when the mean similarity increasingly rises between the new sample and given fault classes.

Step 3: particle update. Update the velocity and position of each particle according to Eqs. (4) and (5).

Step 4: global optimization status checking. If stopping criteria is satisfied, go to step 5. Otherwise, set iteration variable: $t = t + 1$, go to step 2.

Step 5: end global optimization. Finish global optimization, and output global optimized parameters, after which these parameters are considered as initial parameters and then applied to start local optimization in step 6.

Step 6: initialization of local optimization. Set up initial points x_0 (i.e., α, β, and γ obtained from PSO), initial matrix $H_0 = I_0$, iteration variable $k = 0$, max iteration number k_{max}, and then perform the training process from step 7 -10.

Step 7: calibration of search direction. Initialize direction d_k corresponding to Eqs. (13).

Step 8: line-search performance. At each step of this performance, the line-search method searches the best solution (containing the current point, x_k) parallelling to current search direction according to Eqs. (12).

Step 9: local optimization status checking. To evaluate the minimum desired value, F_{fit} is applied according to Eqs. (14) and (15). If precision is satisfied, go to step 11. Otherwise, judge if the current value of k meets the value of k_{max}. If in next iteration $k + 1 = k_{max}$, go to step 7, and set $x_0 = x_{k_{max}}$. Otherwise, go to step 10.

Step 10: Hessian updating with BFGS. Update positive definite symmetric matrix H_{k+1} and search direction d_{k+1} according to Eqs. (9) - (13), and then go to step 7.

Step 11: end local optimization. Finish the overall training procedure and output the optimized parameters, namely α, β, and γ after global and local optimizations.

III. Proposed Methodology for FDD

In general, statistical signal analysis of FDD after signal processing can be mapped into three key phrases: (1) feature extraction; (2) fault classification; (3) fault identification. In this section, the proposed methodology for FDD of roller bearing is presented, including feature selection of statistical parameters, fault classification, and fault identification.

A. Feature selection of statistical parameters

In practical, time-domain statistical parameters have been successfully adopted as trend parameters attempting to reflect the different amplitude and distribution of time-domain signals, by which an enormous amount of information can be obtained from vibration signals. In this paper, before the step of feature extraction using determined features, the widely used time-domain statistical parameters are applied, each performance of which is investigated for extracting features from wavelet coefficients and generating fault signatures in feature space dimension (i.e., the peak value, Root Mean Square (RMS), crest factor, kurtosis, clearance factor, impulse factor, shape factor, and skewness [20]). Apart from that, wavelet Power Spectrum Density (PSD) is also analyzed, which is used for determining the distribution of energy by calculating the absolute-value squared of wavelet coefficients. In addition, rotating speed is considered one of the most critical parameters that has great influences on the performance of statistical parameters. In this study, for obtaining reduced and appropriate parameters for feature extraction and the generation of multi-speed fault signatures, two capabilities of parameters were evaluated, namely speed sensitivity and discriminatory potentials. Obviously for generating discriminatory fault signatures, parameters with low speed sensitivity and high discriminatory ability can be considered as proper indicators for the purpose of distinguishing fault symptoms in high efficiency. For this purpose, the objective functions used are the values of statistical parameters. Hence, the effect of different speeds on 9 statistical parameters above mentioned is firstly evaluated. In this step, standard deviation and linear normalization are used to make the comparison of the performance of 9 feature candidates when they are applied to discriminate fault symptoms after wavelet decomposition under different speeds. Furthermore, for generating fault signatures, the larger deviation between parameters' values can be considered that has better performance to visually distinguish four conditions of roller bearing under different speeds. In this paper, the normalized mean value of 9 candidates was primarily calculated to analyze the discriminatory ability under different speeds, the experimental results of which were presented in Section IV. After that, desired parameters were selected as proper features which were later used for representing vibration signals and generating multi-fault signatures. After evaluation, in this paper, reduced three-dimensional feature space dimension was finally adopted, namely RMS [21], kurtosis [22], [23], and PSD [24], which have relatively better discriminatory performance for effectively generating 2D and 3D fault signatures.

$$RMS = \sqrt{\frac{1}{N}\sum_{i=1}^{N}(x(i)-\bar{x})^2} \tag{16}$$

$$kurtosis = \frac{\frac{1}{N}\sum_{i=1}^{N}(x(i)-\bar{x})^4}{RMS^4} \tag{17}$$

$$PSD = \sum_{i=1}^{N}|x(i)|^2 \tag{18}$$

where $x(i)$ is the ith order of wavelet coefficients ($i = 1, 2, \cdots, N$), $\bar{x}$ denotes the mean value of the wavelet coefficients. In this study, RMS and PSD are used to generate single-speed fault signatures for roller bearing with four conditions in 2D feature space dimension. PSD, RMS, and kurtosis are together adopted to produce multi-speed fault signatures in 3D feature space dimension.

B. Fault classification

Taking different conditions of roller bearing into consideration, the classification of this kind of fault is multi-class classification problem. NN algorithm is one of the most fundamental and commonly used methods for classification [25], which enables to consistently achieve high performance. The basic idea behind NN method is that a new sample can be classified by calculating the similarity distance between this new sample and given classes, after which the group label of this sample can be determined using a class with the nearest similarity distance between this sample. To be more specific, the minimum distance between a undetermined sample and a class may have the greatest similarity compared with other classes. On this basis, a NN-based classification using Mahalanobis distance is therefore adopted in this study for fault classification by mapping new samples into the best matching classes in both training and testing phrases [26].

Suppose that training data set has c classes of feature sets, $w_1, w_2, \cdots, w_t$ is $\{p_t^{i,k}, t = 1, 2, \cdots, c; i = 1, 2, \cdots, N_t; k = 1, 2, \cdots, m\}$, where feature set w_t is the tth class in input data, $p_t^{i,k}$ is the ith row in feature set w_t and the kth feature in this row, m is the sum of samples in each row, i corresponding to N_t, N_t is the row number of w_t, which means for each class of bearing, w_t, has in total N_t number of rows. Suppose each feature set w_t has Sum_t number of samples in total.

The major process of multi-fault classification is described as follows:

step 1: In training step, calculate the average feature set in w_t , namely the mean value of each parameter in feature vector t, can be defined below:

$$\bar{w_t} = \frac{\sum_{k=1}^{m}\sum_{i=1}^{N_t} p_t^{(i,k)}}{Sum_t} \tag{19}$$

step 2: calculate the distance between a new sample s and each average feature set $\bar{w_t}$ using Mahalanobis distance.

$$d_t = \sqrt{(s-\bar{w_t})S^{-1}(s-\bar{w_t})^T} \tag{20}$$

where S^{-1} is covariance matrix resulted from s and $\bar{w}_t$.
step 3: locate the minimum distance d_{min} between sample s and $\bar{w}_t$, and then perform fitness evaluation corresponding to Eqs. (14) and (15). After that, the category label of this sample can be determined using a class having the minimum fitness value, which means high trust rate and low classification error. It is needed to note that step 1 only needs to be computed once in training phrase to decide the vector center of each class. During testing phrase, only step 2 - 3 are needed to calculate the Mahalanobis distance and carry out classification. Additionally, in testing phrase, classification accuracy criteria is applied which can be defined as follows:

$$E_A = \left(\frac{N_f}{N_t + N_f} \right) \times 100\% \tag{21}$$

where N_t and N_f respectively denote the number of true and false classification samples. The classification result with low classification error produces high accuracy approaching to 100%.

C. Fault identification

The aggressive adoption of techniques for machine condition monitoring and pattern recognition has helped in laying the foundation for incipient FDD of roller bearing. The main phrases involved in fault detection and identification include: data acquisition, signal analysis, and fault identification. To be more specific, data acquisition is used to collect physical signals of interest to be analyzed, which is supposed to be correctly operated and measured. Signal analysis is commonly composed of data preprocessing, signal processing, and feature extraction. Fault identification generally includes feature evaluation, and fault classification. Through combining statistical techniques, both of these steps have respective advantages and great influences on the fault diagnosis of rotating components in industrial factories.

In this paper, a novel hybrid diagnosis approach for identifying defects in roller bearings is proposed based on wavelet analysis, reduced three-dimensional feature extraction, statistical similarity analysis. Optimized IMCWT is first obtained by using PSO and quasi-Newton minimization techniques, and later is used to decompose vibration signals obtained from roller bearings. Afterwards, three features, namely PSD, RMS, and kurtosis, are applied for characterizing fault symptoms in wavelet coefficients. After that, NN-based classifier using Mahalanobis distance is adopted for fault classification. On the basis of these techniques, the diagram for bearing fault diagnosis is formed, as illustrated in Fig. 2, the process is described as follows:

Step 1: collect vibration signals from different conditions of roller bearing by using an experimental test rig, and then spilt data into two data sets to respectively prepare training data set and testing data set.
Step 2: signals are normalized to make the signals comparable regardless of differences in magnitude using the following equation:

$$X_i = \frac{x - \bar{x}}{\sigma} \tag{22}$$

where x is the ith element in a signal, $\bar{x}$ and σ are the mean and standard deviation of the vector respectively.
Step 3: initialize three parameters (α, β, and γ) in CWT transformation using impulse model.
Step 4: perform feature extraction using statistical parameters, in this paper, kurtosis, RMS, and PSD are used for this purpose.
Step 5: classify samples into classes by using NN-based classification method with Mahalanobis distance, and then perform fitness evaluation, F_{fit}, between four given classes and the new sample corresponding to Eqs. (14) and (15).
Step 6: go to global and local optimization algorithm. In this phrase, IMCWT model can be used to perform wavelet analysis with three optimized parameters, before the optimization step of which trust rate evaluation is used to select the best wavelet order according to Eqs. (15). Combining optimized IMCWT model, step 3 - 5 can be used for testing classification accuracy based on this approach by using testing data sets. After that, if results can achieve high accuracy this proposed approach can be used for either off-line or on-line fault diagnosis of roller bearing based on optimized IMCWT model.

IV. Experimental Study

In this section, to illustrate the effectiveness of the proposed approach, the fault diagnosis of roller bearing is studied and verified by using a test rig. Primarily, comparison study is carried out for evaluating the different performances of statistical parameters and vector distances, which are critical for generating discriminatory multi-speed fault signatures. Afterwards, the experimental results of bearing diagnosis and the generation of fault signatures are investigated and presented based on the proposed approach in this paper.

A. Experimental System Description

In this study, PT 500 machinery diagnostic system [27] is used to collect vibration signals of four conditions of roller bearing, as shown in Fig. 3 (a) and (b). Roller bearing faults kit is composed of motor assembly, motor control unit, shaft, four types of bearings, belt drive kit, and computerised vibration analyser. The control unit is used to collect speed and horsepower data. The piezo-electric sensor and measurement amplifier are used for acceleration measurement. During the tests, vibration data were captured at a sampling frequency of 8 kHz for different bearing conditions. Roller bearings used in this paper are illustrated in Fig. 4, which are bearing A without damage, bearing B with outer race damage, bearing C with inner race damage, and bearing D with rolling element damage. To study and evaluate the performance of this proposed approach, four conditions of roller bearing were monitored and respectively recorded under five rotating speeds. That is, 1000, 1500, 2000, 2500, and 3000 r.p.m.

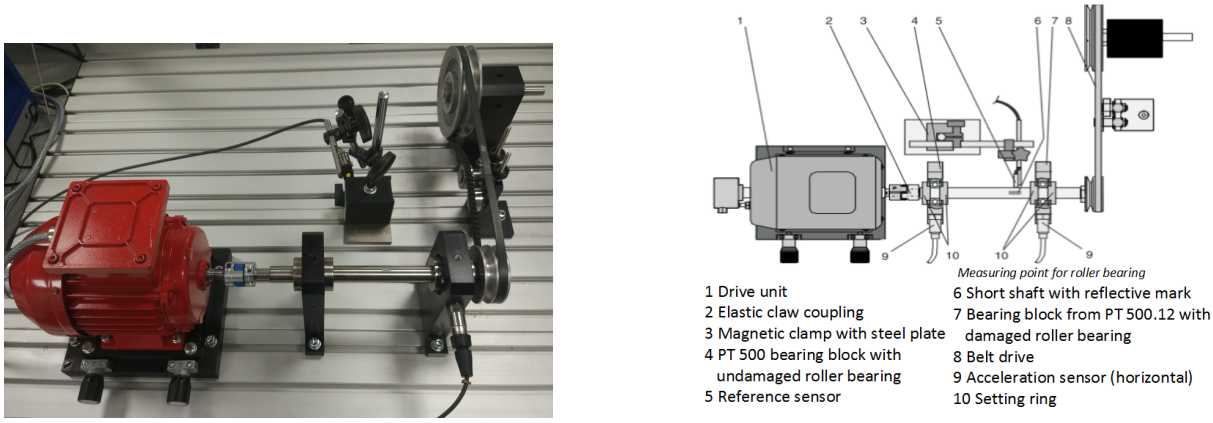

(a) PT 500 test rig (b) layout graph of test rig [27]

Fig. 3: PT 500 experimental test rig and corresponding layout graph.

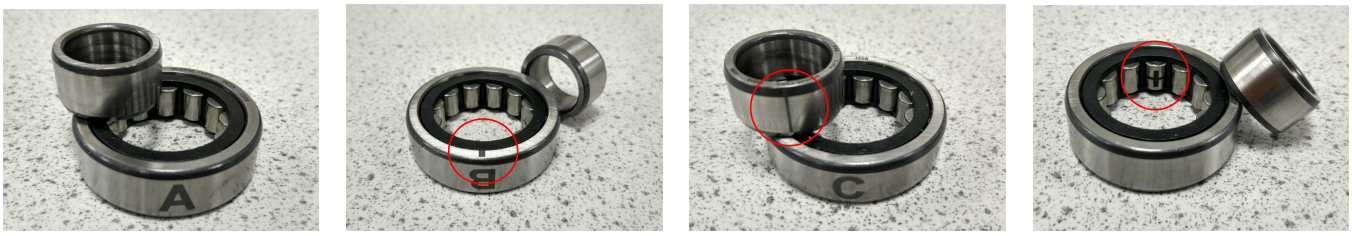

(a) Normal bearing A as reference (b) Bearing B with outer race defect (c) Bearing C with inner race defect (d) Bearing D with roller defect

Fig. 4: One normal condition and three faulty conditions of roller bearings used in this study.

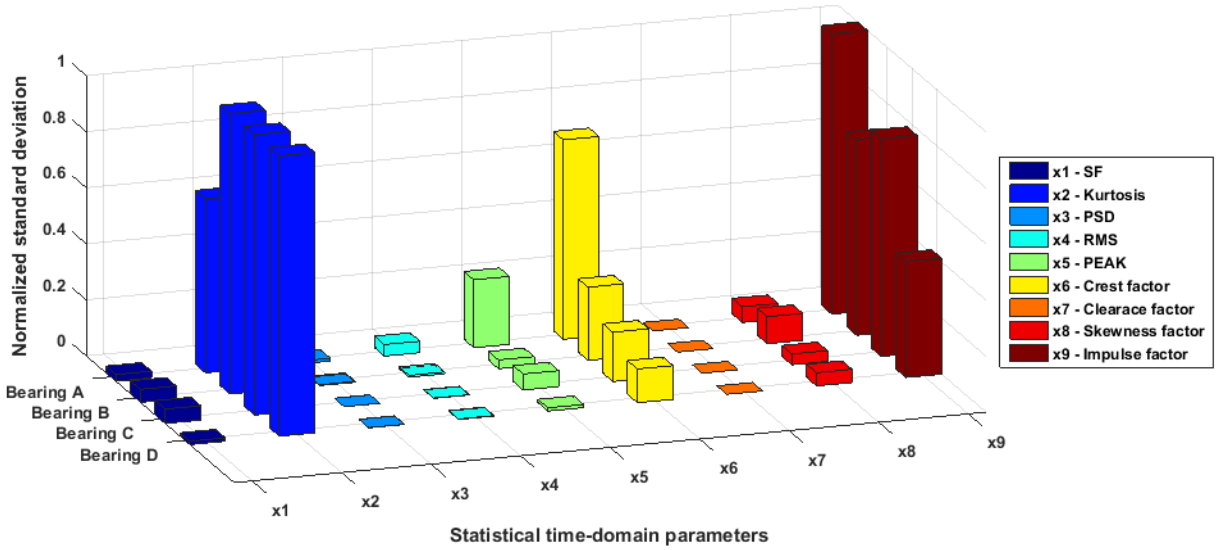

Fig. 5: The deviation of statistical parameter values under different speeds (i.e., 500 and 3000 r.p.m) using linear normalization.

The experimental data sets contain four conditions of roller bearing, for each condition in one speed, 200 data sets are used, and therefore the total number of data sets corresponding to four roller bearings are 800. In each data set, 4096 sampling points are used. Finally, the entire data set is split into two categories, namely 400 for training and 400 for testing respectively.

B. Experimental Results

1) Analysis of statistical parameters and distance functions for fault diagnosis: In this paper, before determining reduced three-dimensional features, widely used statistical parameters were firstly analyzed to select proper candidates with high discriminatory ability and performance which would be ap-

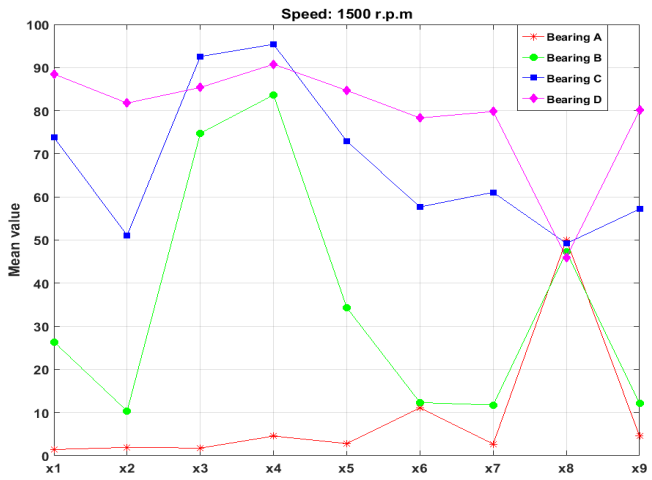

(a) Mean values of the statistical parameters with 1500 r.p.m

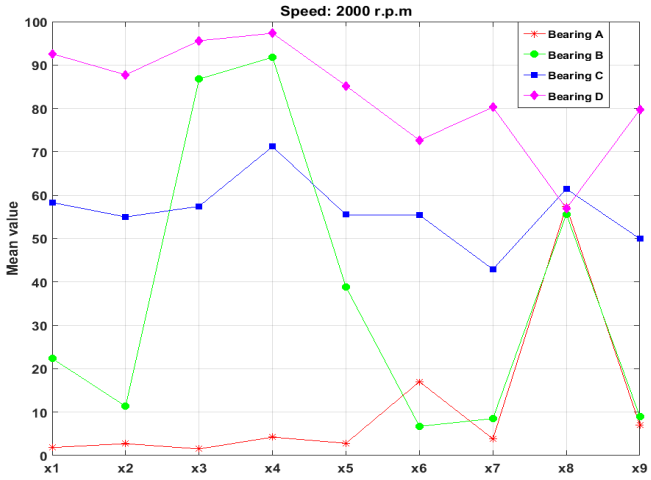

(b) Mean values of the statistical parameters with 2000 r.p.m

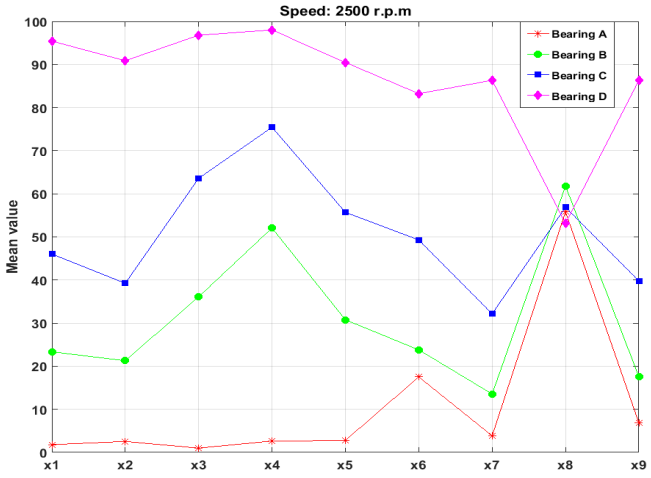

(c) Mean values of the statistical parameters with 2500 r.p.m

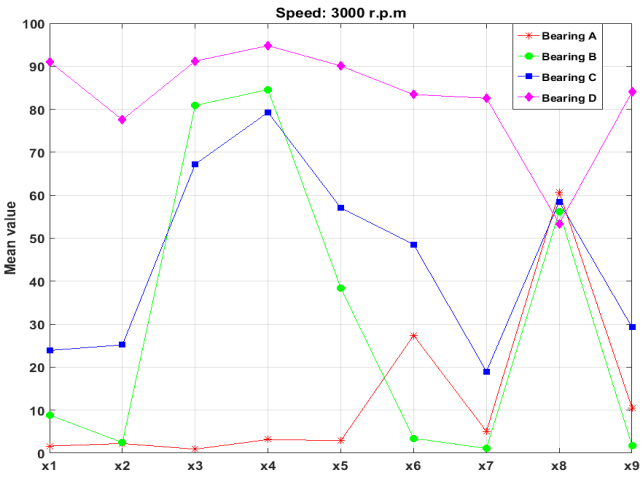

(d) Mean values of the statistical parameters with 3000 r.p.m

Fig. 6: The discriminatory ability of statistical parameters representing roller bearings under different rotating speeds. (The parameters represented by $x1$ - $x9$ refer to Fig. 5.)

TABLE I: The comparative results of vector distance using three speed data sets: 1000, 2000, and 3000 r.p.m.

Vector distance	Bearing A trust rate(%)	Bearing B trust rate(%)	Bearing C trust rate(%)	Bearing D trust rate(%)	Mean trust rate (%)	Testing accuracy (%)
Mahalanobis	99.15	86.46	96.69	95.48	94.45	100
Euclidean	98.94	84.29	91.10	95.36	92.42	100
CityBlock	99.16	77.79	94.61	95.86	91.86	100
Chebyshev	97.35	91.77	80.00	92.48	90.40	100

plied to generate multi-speed fault signatures. For this purpose, in total 9 statistical parameters were primarily investigated to extract fault symptoms under two rotating speeds, 500 and 3000 r.p.m respectively. These 9 parameters are represented from $x_1, x_2, \cdots, x_9$, including shape factor, kurtosis, PSD, RMS, peak, crest factor, clearance factor, skewness factor, and impulse factor. In this study, taking into account that four conditions of roller bearing and two speeds, there are in total 1600 data sets were used to compare their performance. The second-scale Morlet wavelet was chosen for the application of wavelet transform, after which statistical parameters were used to extract features, and then standard deviation was applied to evaluate the dispersion degree of each parameter in same bearing condition and speed. From Fig. 5, it can be concluded that kurtosis, crest factor, and impulse factor are the most sensitive parameters for detecting incipient faults

TABLE II: Single-speed resulting trust rate of fault detection and identification on roller bearing

Single speed	Bearing A trust rate(%)	Bearing B trust rate(%)	Bearing C trust rate(%)	Bearing D trust rate(%)	Mean trust rate (%)	Testing accuracy (%)
1000	99.77	98.36	96.17	99.74	98.52	100
1500	99.75	99.44	98.40	99.79	99.35	100
2000	99.75	99.46	99.44	98.50	99.28	100
2500	99.85	99.92	99.58	99.66	99.75	100
3000	99.70	97.47	80.00	98.58	97.03	100

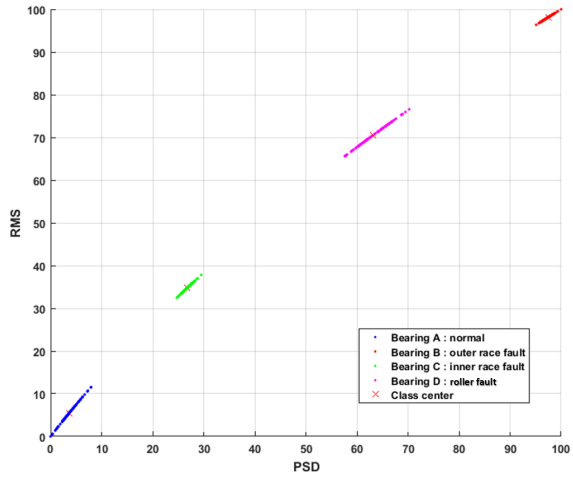

(a) Distribution of data sets at 1000 r.p.m

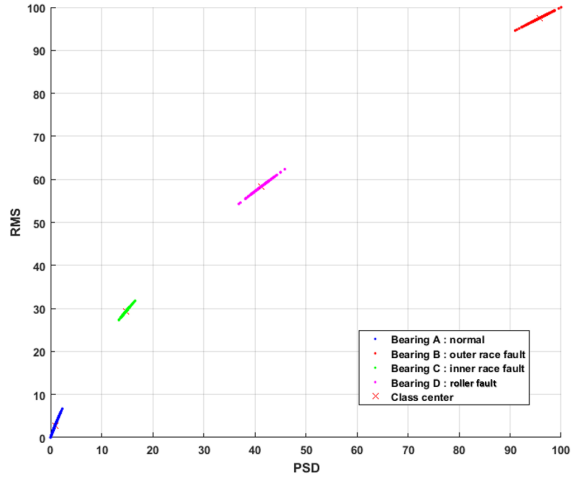

(b) Distribution of data sets at 1500 r.p.m

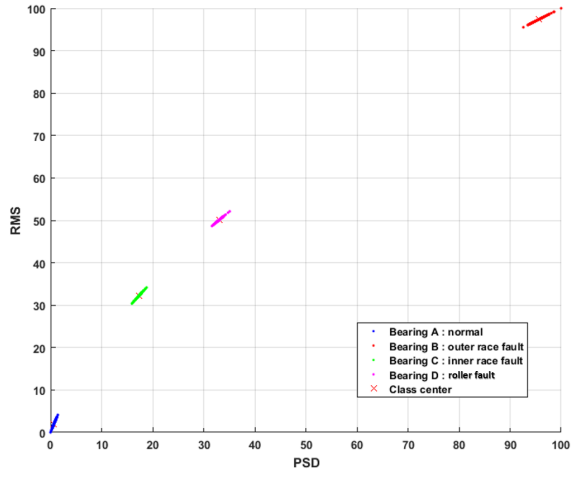

(c) Distribution of data sets at 2500 r.p.m

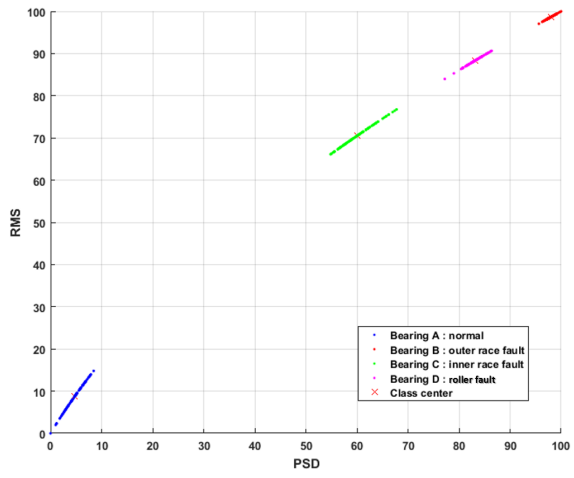

(d) Distribution of data sets at 3000 r.p.m

Fig. 7: The 2D fault signatures (based on RMS and PSD) with single-speed showing training data distribution.

corresponding to increasing speeds in this study. For the purpose of generating multi-speed fault signatures, sensitive parameters however are not the proper candidates since the mean value of which would increasingly change following with the increasing speed, as a result of which these parameters may be probably too sparse to represent one sample in feature space dimension. Less sensitive parameters therefore were chosen in this study, among those shape factor, PSD, RMS, and clearance factor are both considered as appropriate candidates to draw fault signatures. It is needed to note that both of these parameters perform well in feature extraction, in this study only reduced three-dimensional feature space is considered for

TABLE III: Multi-speed resulting trust rate of fault detection and identification on roller bearing

Number of speed	Speeds	Number of training data sets	Number of testing data sets	Number of misclassified data sets	Trust rate	Testing accuracy(%)
1	1000	400	400	0	98.94	100
2	1000,1500	800	800	0	98.38	100
3	1000,1500,2000	1200	1200	0	94.45	100
4	1000,1500,2000,2500	1600	1600	0	91.77	100
5	1000,1500,2000,2500,3000	2000	2000	0	91.10	100

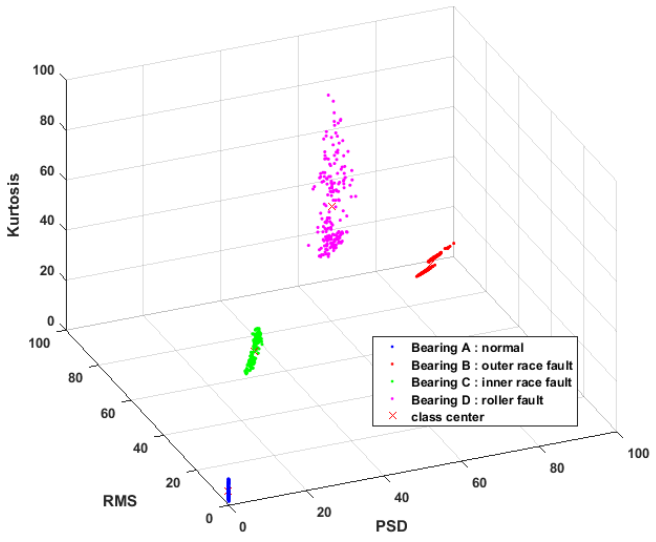

(a) Distribution of data sets at 1000, and 1500 r.p.m

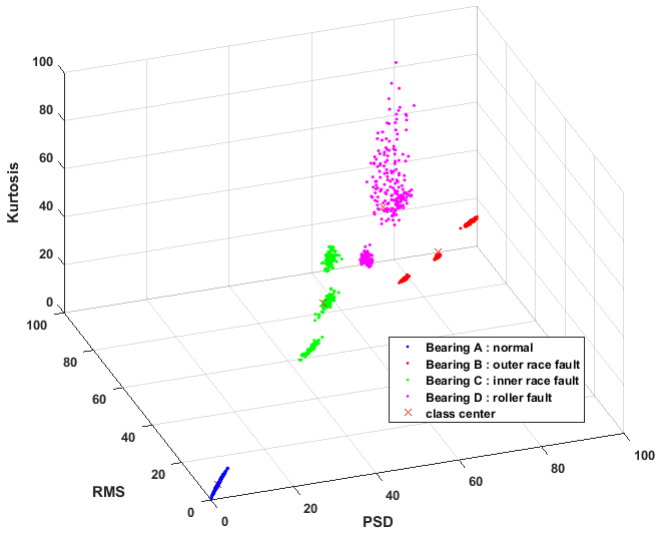

(b) Distribution of data sets at 1000, 1500, and 2000 r.p.m

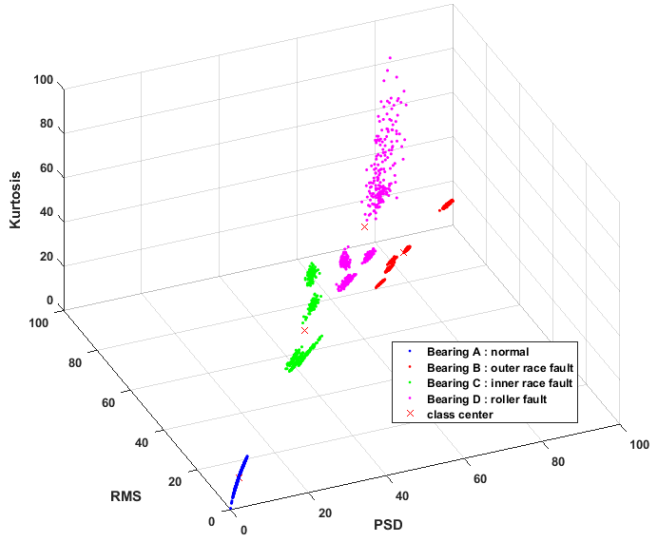

(c) Distribution of data sets at 1000, 1500, 2000, and 2500 r.p.m

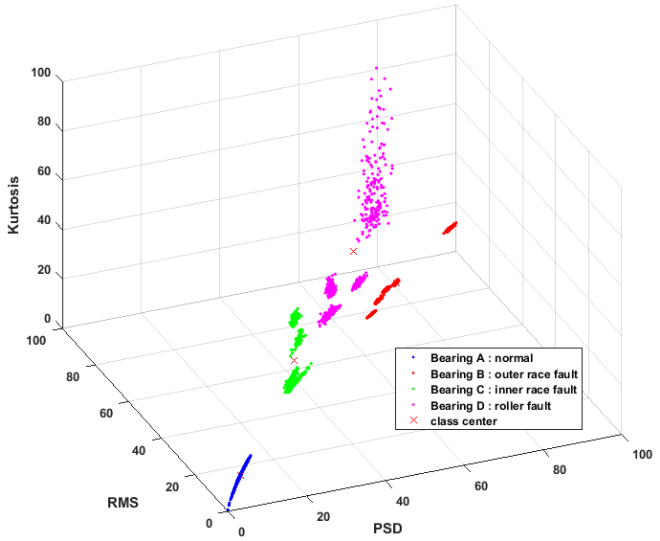

(d) Distribution of data sets at 1000, 1500, 2000, 2500, and 3000 r.p.m

Fig. 8: The 3D fault signatures (based on RMS, PSD and kurtosis) with multi-speed showing training data distribution.

fault feature extraction and generation of fault signatures. That is, each coefficient after wavelet decomposition is represented by its three-dimensional feature vector.

Additionally, the ability of discriminatory potential of each statistical parameter was evaluated by making comparison between mean values of statistical parameters when used to achieve better separability representing four bearing conditions. Four rotating speeds (i.e., 1500, 2000, 2500 and 3000

TABLE IV: Classification accuracy comparison by using CWT with different kernels under five different speeds

Operating wavelet	Number of resolution level	Number of testing data sets	Number of misclassified	Trust rate (%)	Testing accuracy (%)
IMCWT	4	2000	0	94.60	100
Daubechies2	3	2000	0	90.45	100
Daubechies4	3	2000	0	89.79	100
Daubechies10	3	2000	0	87.57	100
Mexican hat	1	2000	3	87.23	99.85
Haar	3	2000	6	88.39	99.72
Meyer	3	2000	28	70.22	98.60
Morlet	3	2000	42	83.41	97.90

r.p.m) and in total 3200 data sets were tested in this study, the result of which is illustrated in Fig. 6. From this figure, it can be seen that parameters in the left side can relatively discriminate four bearing conditions after normalization from 0 to 100. To be more specific, four bearing conditions can be separately represented by one parameter with different values after normalization. Hence, comprehensively taking speed sensitivity and discriminatory potential into account, in this proposed study, PSD, RMS are selected as features to generate 2D fault signatures. Moreover, it can be seen from Fig. 5 that kurtosis is highly sensitive to variation of rotating speed, which is an appropriate feature that can be used to transfer 2D feature space to 3D dimension when multi-speed signals involved for fault diagnosis. Therefore, through combining kurtosis, RMS, and PSD together, this three-dimensional feature space can be properly applied to generate multi-speed fault signatures in 3D feature space dimension. In addition, to illustrate the selected distance function, Mahalanobis that has better performance in NN-based classification, commonly used vector distances (e.g., Euclidean, City Block, and Chebyshev) were selected to evaluate similarity between the new sample and given classes. Trust rate and classification accuracy were applied to evaluate the classification results corresponding to Eqs. (14) and (19). As shown in Table I, it can be seen that both of four distances can achieve 100% accuracy. Mahalanobis analysis however achieved more high trust rate than the rest. That is, the mean similarity between correct classification and samples evaluated by Mahalanobis distance is more relatively accurate than the others. According to the literatures, different from other similarity distances, Mahalanobis distance takes the correlations of data sets into account. Hence, Mahalanobis distance used for statistical similarity analysis is more unitless and scale-invariant.

2) Experimental results of multi-speed fault diagnosis and signatures: After having determined the feature vector and vector distance method, original vibration data sets of roller bearing were used to verify the effectiveness of this proposed approach and multi-speed fault signatures. Primarily, the classification accuracy of single-speed diagnosis and the fault signatures are illustrated in Fig. 7 and Table II. Fig. 7 shows the 2D data distribution plots of the samples under a single speed in this study. It can be noticed that the training data sets with fault symptoms can be clearly found in the right half, which visually seems like "fault trajectory" that can be regarded to single-speed fault signatures. The healthy samples are represented by blue points in the lower left corner.

In addition, the experimental results of multi-speed fault diagnosis and 3D fault signatures are summarized in Table III and Fig. 8. Different from single-speed result, it can be seen that in Fig. 8 samples representing one condition is consisted with various groups corresponding to the number of rotation speeds used in the training phrase. Interestingly, for both single or multi speed fault signatures, the healthy condition (represented by blue color) intensively locates in the lower left corner with an intensive manner. However, when two rotating speeds of 1000 and 1500 r.p.m used for fault signatures, samples representing roller fault condition (represented by pink color) approximately locate together in the feature space. In conclusion, it can be noticed that fault signatures generated using this proposed method can be used to accurately recognize whether the current running state of roller bearing is healthy. Moreover, most of the time, samples would be normally labeled with a certain rotating speed in training phrase. Nevertheless, sometimes it can not achieve high accuracy when the speed of sample can not be tested and determined. In this paper, from Fig. 7 and Fig. 8 it is shown that multi-fault signatures provide a visualized solution that can be used to classify samples to certain groups and meanwhile estimate current speed of testing samples by comparing with the data distribution plots in feature space.

Additionally, the comparative performances of wavelet analysis using different wavelet kernels are illustrated in Table IV. Each best scale of wavelet transform was selected according to fitness evaluation Eqs. (15), which is used to evaluate the mean statistical similarity between testing samples and given classes. It can be seen that both of IMCWT model and Daubechies 2/4/10 wavelets can achieve 100% classification success rate; however, misclassified samples occurred when the rest are used. Moreover, it shows that IMCWT model enables to obtain the highest trust rate used for five-speed fault diagnosis in contrast with the rest. In addition, to manifest the efficiency of the proposed approach, recent bearing diagnosis works on bearings based on wavelet analysis published in literatures have been reviewed in Table V. In this table,

TABLE V: Comparative review of related methods and the proposed approach for bearing fault diagnosis

	Abbasion et al. [11]	Paya et al. [12]	Kankar et al. [14]	Lou et al. [15]	Konar et al. [16]	Present Work
Objects	Roller bearings	Bearings and gears	Roller bearings	Ball bearings	Ball bearings	Roller bearings
Defects considered	Bearing looseness,defects in bearing raceways and roller element	Defects on inner race of bearing and gear tooth irregularity	Spall in inner race, outer race, rolling element and combined component defects	Defects on inner race and ball element	Healthy motor and faulty motor with faulted bearing	Defects on inner race, outer race and roller element
Techniques used for fault diagnosis	Meyer wavelet	Daubechies 4	Meyer, Coiflet5, Symlet2, Gaussian,complex Morlet and Shannon wavelets	Daubechies 2 and 10	Morlet and Daubechies 10	Adaptive impulse modelling based wavelet
Features considered	Fundamental cage frequency, inner raceway frequency, outer raceway frequency and ball rotational frequency	10 wavelet numbers indicating both time and frequency and their 10 corresponding amplitudes	Kurtosis, skewness and standard deviation corresponding to scale maximizing energy to Shannon entropy ratio	Standard deviation ratio using the standard deviation as reference	Root mean square (RMS), crest factor and kurtosis	Root mean square (RMS), wavelet power spectrum density (PSD), and kurtosis
Classifier used	Support vector machine	Artificial neural networks	Support vector machines, artificial neural networks, self-organizing maps	Neural fuzzy inference	Support vector machine	Statistical similarity analysis with NN-based classifier using Mahalanobis distance
Classifier accuracy	100%	96%	98.67%	NA	Wavelet scale: 1-8: 100%; 1-15: 96.67%	100%

comparison has been conducted based on the perspectives of objects adopted, defects considered, techniques used for fault diagnosis, features considered, classification method used, and the classification efficiencies in each paper.

V. Conclusion

In this paper, a novel hybrid fault diagnosis methodology is presented, for roller bearings under multi-speed operations. In the proposed approach, IMCWT is applied to extract fault information hidden in the vibration signals, by providing high time-frequency resolution in the signal processing stage. A reduced three-dimensional feature space, based on statistical parameters (i.e., RMS, PSD, and kurtosis), is adopted to extract fault features after the wavelet decomposition. Then, a NN-based classifier based on Mahalanobis distance is used to evaluate the similarity between samples and give classes for identifying the conditions of the testing samples. Finally, the effectiveness of the proposed method is demonstrated through experimental trials.

An overall accuracy of 100% is achieved in the experimental results, which has demonstrated that the proposed approach can effectively classify vibration signals of four roller bearing conditions, i.e., healthy bearing and defective bearings with fault on the inner race, outer race, and roller element. In addition, it can be evidently seen that this method is capable to provide discriminatory fault signatures for both single-speed and multi-speed data sets, which has shown a great scope of extending this technique in identifying other types of rotating mechanical faults.

Acknowledgement

This work is partially supported by National Natural Science Foundation of China (NO.61401107), International and Hong Kong, Macao & Taiwan collaborative innovation platform and major international cooperation projects of colleges in Guangdong Province (No.2015KGJHZ026), The Natural Science Foundation of Guangdong Province (No.2016A030307029), Guangdong University of Petrochemical Technology Internal Project 2012RC106.

References

[1] J. Chen, Z. Li, J. Pan, G. Chen, Y. Zi, J. Yuan, B. Chen, and Z. He, "Wavelet transform based on inner product in fault diagnosis of rotating machinery: a review," *Mechanical systems and signal processing*, vol. 70, pp. 1–35, 2016.

[2] J. Huang, G. Chen, L. Shu, S. Wang, and Y. Zhang, "An experimental study of clogging fault diagnosis in heat exchangers based on vibration signals," *IEEE Access*, vol. 4, pp. 1800–1809, 2016.

[3] P. Tavner, "Review of condition monitoring of rotating electrical machines," *IET Electric Power Applications*, vol. 2, no. 4, pp. 215–247, 2008.

[4] M. A. Abu-Zeid and S. Abdel-Rahman, "Bearing problems effects on the dynamic performance of pumping stations," *Alexandria Engineering Journal*, vol. 52, no. 3, pp. 241–248, 2013.

[5] M. Kang, M. R. Islam, J. Kim, J.-M. Kim, and M. Pecht, "A hybrid feature selection scheme for reducing diagnostic performance deterioration caused by outliers in data-driven diagnostics," *IEEE Transactions on Industrial Electronics*, vol. 63, no. 5, pp. 3299–3310, 2016.

[6] Y. Zhang, C. Bingham, Z. Yang, B. W.-K. Ling, and M. Gallimore, "Machine fault detection by signal denoisingwith application to industrial gas turbines," *Measurement*, vol. 58, pp. 230–240, 2014.

[7] B. Kim, S. Lee, M. Lee, J. Ni, J. Song, and C. Lee, "A comparative study on damage detection in speed-up and coast-down process of grinding spindle-typed rotor-bearing system," *Journal of materials processing technology*, vol. 187, pp. 30–36, 2007.

[8] C. Torrence and G. P. Compo, "A practical guide to wavelet analysis," *Bulletin of the American Meteorological society*, vol. 79, no. 1, pp. 61–78, 1998.

[9] M. M. Tahir, A. Q. Khan, N. Iqbal, A. Hussain, and S. Badshah, "Enhancing fault classification accuracy of ball bearing using central tendency based time domain features," *IEEE Access*, 2016.

[10] H. Hong and M. Liang, "Fault severity assessment for rolling element bearings using the Lempel–Ziv complexity and continuous wavelet transform," *Journal of sound and vibration*, vol. 320, no. 1, pp. 452–468, 2009.

[11] S. Abbasion, A. Rafsanjani, A. Farshidianfar, and N. Irani, "Rolling element bearings multi-fault classification based on the wavelet denoising and support vector machine," *Mechanical Systems and Signal Processing*, vol. 21, no. 7, pp. 2933–2945, 2007.

[12] B. Paya, I. Esat, and M. Badi, "Artificial neural network based fault diagnostics of rotating machinery using wavelet transforms as a preprocessor," *Mechanical systems and signal processing*, vol. 11, no. 5, pp. 751–765, 1997.

[13] J. Zarei, M. A. Tajeddini, and H. R. Karimi, "Vibration analysis for bearing fault detection and classification using an intelligent filter," *Mechatronics*, vol. 24, no. 2, pp. 151–157, 2014.

[14] P. Kankar, S. C. Sharma, and S. Harsha, "Fault diagnosis of ball bearings using continuous wavelet transform," *Applied Soft Computing*, vol. 11, no. 2, pp. 2300–2312, 2011.

[15] X. Lou and K. A. Loparo, "Bearing fault diagnosis based on wavelet transform and fuzzy inference," *Mechanical systems and signal processing*, vol. 18, no. 5, pp. 1077–1095, 2004.

[16] P. Konar and P. Chattopadhyay, "Bearing fault detection of induction motor using wavelet and support vector machines (SVMs)," *Applied Soft Computing*, vol. 11, no. 6, pp. 4203–4211, 2011.

[17] E. Schukin, R. Zamaraev, and L. Schukin, "The optimisation of wavelet transform for the impulse analysis in vibration signals," *Mechanical Systems and Signal Processing*, vol. 18, no. 6, pp. 1315–1333, 2004.

[18] J. Kennedy, "Particle swarm optimization," in *Encyclopedia of machine learning*. Springer, 2011, pp. 760–766.

[19] R. Battiti and F. Masulli, "BFGS optimization for faster and automated supervised learning," in *International neural network conference*. Springer, 1990, pp. 757–760.

[20] D. Dyer and R. Stewart, "Detection of rolling element bearing damage by statistical vibration analysis," *Journal of mechanical design*, vol. 100, no. 2, pp. 229–235, 1978.

[21] A. Nabhan, M. Nouby, A. Sami, and M. Mousa, "Multiple defects detection in outer race of gearbox ball bearing using time domain statistical parameters," *International Journal of Vehicle Structures & Systems*, vol. 8, no. 3, p. 167, 2016.

[22] Y. Wang, J. Xiang, R. Markert, and M. Liang, "Spectral kurtosis for fault detection, diagnosis and prognostics of rotating machines: A review with applications," *Mechanical Systems and Signal Processing*, vol. 66, pp. 679–698, 2016.

[23] J. Tian, C. Morillo, M. H. Azarian, and M. Pecht, "Motor bearing fault detection using spectral kurtosis-based feature extraction coupled with k-nearest neighbor distance analysis," *IEEE Transactions on Industrial Electronics*, vol. 63, no. 3, pp. 1793–1803, 2016.

[24] J. CusidÓCusido, L. Romeral, J. A. Ortega, J. A. Rosero, and A. G. Espinosa, "Fault detection in induction machines using power spectral density in wavelet decomposition," *IEEE Transactions on Industrial Electronics*, vol. 55, no. 2, pp. 633–643, 2008.

[25] T. Cover and P. Hart, "Nearest neighbor pattern classification," *IEEE transactions on information theory*, vol. 13, no. 1, pp. 21–27, 1967.

[26] Z. Hu, M. Xiao, L. Zhang, S. Liu, and Y. Ge, "Mahalanobis distance based approach for anomaly detection of analog filters using frequency features and parzen window density estimation," *Journal of Electronic Testing*, vol. 32, no. 6, pp. 681–693, 2016.

[27] "PT 500 machinery diagnostic system," (Date last accessed 9-December-2016). [Online]. Available: www.gunt.de/static/s3680_1.php

Zhiqiang Huo is currently working towards his Ph.D. degree at University of Lincoln, UK. He received his Ms. and BS. from China University of Geosciences Beijing, China in 2016 and 2013 respectively. His research interests lie in the field of fault diagnosis of industrial systems, wireless sensor networks, and participatory sensing. He has served as web chairs in international conferences, such as CollaborateCom 2017, AINIS 2015 and 2016.

Yu Zhang is currently a Senior Lecturer in the School of Engineering, University of Lincoln, Lincoln, U.K. She has obtained her BSc degree from School of Aerospace Engineering and Applied mechanics, Tongji University, Shanghai, China, in 2004. She has finished her MSc degree and PhD degree from the Department of Civil Engineering, University of Nottingham, Nottingham, U.K. in 2005 and 2011 separately. Her research interests include Equipment Fault Detection and Diagnosis, Grey-box System Modelling, and development of Data Analysis and Machine Learning algorithms. Her recent major projects, including two Innovate UK projects, one international project with Guangdong University of Petrochemical Technology and one industrial project funded by Siemens, Germany, all focus on the areas of Data Analysis and Machine Fault Diagnosis.

Pierre Francq is currently studying engineering for his Ms. at Mines Albi, University of Toulouse, France. He received his BS. from University of Toulouse in 2015. His fields of interest are supply chain management, lean management and nonlinear programming.

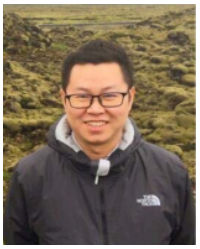

Lei Shu (M07-SM15) is a Lincoln Professor of University of Lincoln, UK and a Distinguished Professor in Guangdong University of Petrochemical Technology. He is also the executive director of Guangdong Provincial Key Laboratory of Petrochemical Equipment Fault Diagnosis, China. His main research field is Wireless Sensor Networks. He has published over 300 papers in related conferences, journals, and books in the area of sensor networks. He had been awarded the Globecom 2010 and ICC 2013 Best Paper Award. He has been serving as Editor-in-Chief for EAI Endorsed Transactions on Industrial Networks and Intelligent Systems, and associate editors for IEEE Systems Journal, IEEE Access, etc. He has served as more than 50 various Co-Chair for international conferences/workshops, e.g., IWCMC, ICC, ISCC, ICNC, Chinacom, especially Symposium Co-Chair for IWCMC 2012, ICC 2012, General Co-Chair for Chinacom 2014, Qshine 2015, Collaboratecom 2017, Mobiquitous2018, Steering and TPC Chair for InisCom 2015; TPC members of more than 150 conferences, e.g., ICDCS, DCOSS, MASS, ICC, Globecom, ICCCN, WCNC, ISCC.

Jianfeng Huang (M'15) received the Ph.D degree from South China University of Technology, Guangzhou, China, in 2016. He currently works in Guangdong University of Petrochemical Technology as an Associate Professor and the Department Head of Safety Engineering. Since 2012, he has been with the Guangdong Petrochemical Equipment Fault Diagnosis Key Laboratory. His research interests include industrial wireless sensor networks, petrochemical equipment fault diagnosis, and safety assessment.